Available online at www.sciencedirect.com
ScienceDirect
Journal of the European Ceramic Society 30 (2010) 3357–3362
www.elsevier.com/locate/jeurceramsoc

A first study of the high-temperature plasticity of ceria-doped zirconia polycrystals

Santiago de Bernardi-Martín [a], Diego Gómez-García [a,*], Arturo Domínguez-Rodríguez [a], Goffredo de Portu [b]

[a] *Departamento de Física de la Materia Condensada, Universidad de Sevilla-ICMSE, CSIC, Apartado 1065, 41080 Sevilla, Spain*
[b] *Institute for Science and Technology of Ceramics (CNR-ISTEC), Faenza, Italy*

Received 30 April 2010; received in revised form 20 July 2010; accepted 28 July 2010
Available online 1 September 2010

Abstract

Ceria–zirconia ceramic alloys were sintered by high-temperature annealing, considering several synthesis temperatures to obtain a full-dense ceria–zirconia ceramic material using a temperature as low as possible. It was found that fully density is achieved at temperatures of 1450 °C.

Monolithic specimens were crept under compression at high temperatures. The creep results fitted an empirical constitutive equation consistent with a classical Ratchinger mechanism for grain switching. This result was confirmed through microstructural characterization of as-received and post-mortem specimens. Since the conventional Ashby–Verrall model is contrary to the mechanism controlling creep in other zirconia alloys, the results are considered in the framework of a new grain boundary sliding model, with particular discussion of the validity of that model for the ceria–zirconia case.

Keywords: CeO_2; ZrO_2; Creep; Deformation mechanism

1. Introduction

Zirconia alloys have been at the forefront of research on ceramic systems during the last three decades. Cerium- and yttrium-doped tetragonal zirconia polycrystals (CeTZP and YTZP, respectively) have been extensively studied due to their having better thermomechanical properties than other zirconia-based ceramics. Yttria–zirconia is well known as having been the first ceramic material known to exhibit superplasticity at moderate temperatures.[1] Since that discovery, an exhaustive effort[2] has been put into attaining a full comprehension of superplasticity from a fundamental standpoint. Despite the numerous publications on the topic, it has only been recently that a consistent theory of ceramic superplasticity applicable to zirconia ceramics has emerged.[3]

Among the factors governing the superplastic response, a key has repeatedly been reported to be the chemical nature at the boundaries. Indeed, yttrium segregation to the boundaries is known to affect the mechanical behaviour,[4] mostly in a negative sense.[5] The crucial point is the formation of an electrically charged layer at the boundaries due to the valence differences between zirconium and yttrium cations. Ceria–zirconia ceramics have as yet not been deemed worthy of any great attention. However, they have been considered in this context as a model system on which to check the strength of electrically charged layers as an obstacle limiting grain mobility. Indeed, for obvious reasons, no charged layers of cation segregations can appear in this system. A systematic study and analysis of the mechanical behaviour of this alloy is currently under way, with the present communication being a report of the pioneering work.

2. Experimental procedure

2.1. Sintering

High purity commercial ceria–zirconia powders with 20 nm average grain size were uniaxially and then cold-isostatically pressed under 300 MPa isostatic pressure. A density equal to 50% the theoretical one was reached prior to sintering. Chemi-

* Corresponding author.
E-mail address: dgomez@us.es (D. Gómez-García).

0955-2219/$ – see front matter © 2010 Elsevier Ltd. All rights reserved.
doi:10.1016/j.jeurceramsoc.2010.07.043

cal analysis of the impurity content was carried out prior to any treatment. The analysis shows the presence of 0.002 wt% SiO_2, 0.005 wt% Fe_2O_3 and 0.018% Na_2O as main impurities. The compacted pieces were heated at 600 °C/h to 1450 °C in a conventional super-kanthal furnace, maintained at that temperature for 30 min, and cooled to room temperature at about the same rate. The recovered specimens were checked to be full-dense by density determination using Archimedes' method. The average grain size, as determined by scanning electron microscopy (SEM) and the subsequent analysis of the grain size distributions, was $1.4 \pm 0.6\ \mu m$.

2.2. Mechanical characterization

The sintered samples were cut into parallelepipeds of dimensions 2.5 mm × 2.5 mm × 5.0 mm for uniaxial compression along the long axis. The machine used was a prototype described elsewhere.[6]

Two sets of experiments were performed: first, creep tests at temperatures from 1200 °C to 1300 °C at a constant stress of 125 MPa; and second, creep tests at a constant temperature (1300 °C) at different stress stages from 28 MPa to 80 MPa. The strain rates in all cases were between $10^{-6}\ s^{-1}$ and $10^{-5}\ s^{-1}$. Data were analyzed using the conventional creep equation:

$$\dot{\varepsilon} = A\frac{Gb}{kT}\left(\frac{\sigma}{G}\right)^n\left(\frac{b}{d}\right)^p D_0 \exp\left(-\frac{Q}{kT}\right) \quad (1)$$

Here, A is a dimensionless constant, G the shear modulus, b the magnitude of the Burgers vector, k Boltzmann's constant, T the absolute temperature, d the grain diameter, σ the applied stress, p and n are usually termed the grain size and stress exponents, respectively, and D_0 is the pre-exponential factor of a diffusion coefficient, with Q being the activation energy of its temperature dependence.

These experiments yielded measured values of the quantities Q (first set of experiments) and n (second set). Both quantities were measured from stress jumps at constant temperature (in the case of n) or temperature changes at constant stress (in the case of Q) to ensure that the microstructure remained constant (i.e. the quantity A is the same). This method prevents the results from being affected by the cross-sectional area increase which occurs during deformation. However, the change of the sample areas affects the stress levels. To account for that effect, the stress are corrected according to the following procedure: since the sample volume is known to remain constant and the deformation is homogeneous, the cross-sectional area depends on the strain through an exponential law: $S = S(\varepsilon = 0)\exp(\varepsilon)$. Thus, the stress should be determined by another exponential law: $\sigma = \sigma(\varepsilon = 0)\exp(-\varepsilon)$. This equation has been taken into account when displaying the stress level for each stage. The stresses displayed are those determined at the onset of each one.

2.3. Microstructural characterization

Both the as-received and post-mortem specimens were characterized by conventional SEM in order to determine the grain size distribution prior to and after deformation. Grain boundaries were optically resolved by SEM after a rapid heat treatment of the previously polished surfaces. All grain size distributions were found to be log-normal. An X-ray diffraction analysis was performed to study the phase composition. Only the tetragonal phase was observed, with a characteristic peak at 29.974°. No monoclinic or cubic peaks appeared in the samples. The grain size distribution was determined from the SEM pictures. The grain diameter was defined as the Feret's diameter.

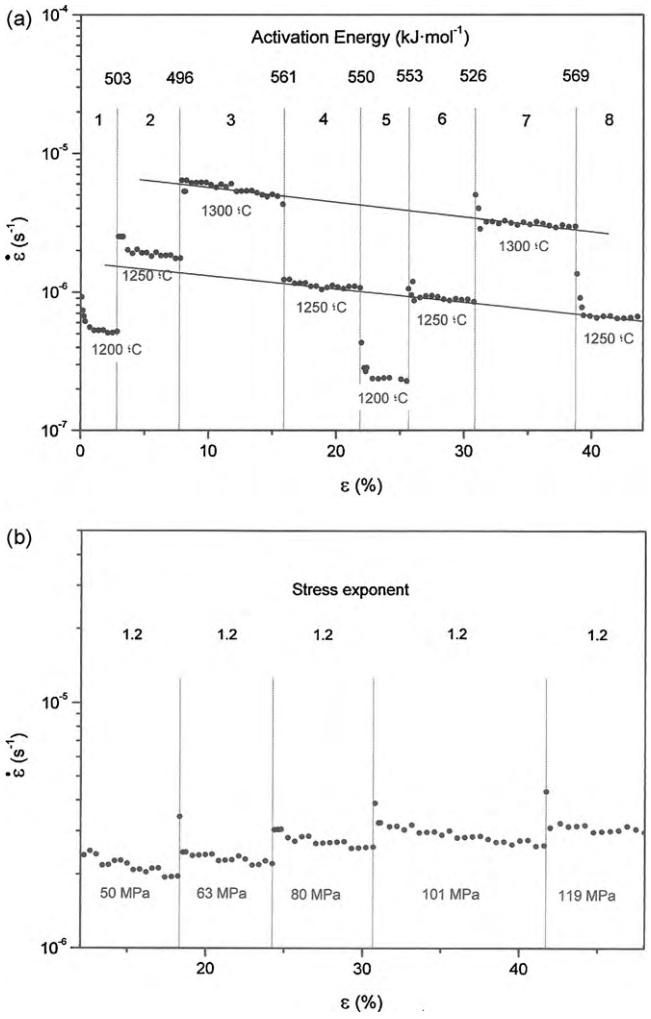

Fig. 1. (a) Strain rate *versus* strain with several temperature jumps. At each stage, the activation energies are given at the top of the plot and the temperatures at the bottom. (b) Strain rate *versus* strain with several stress jumps. At each stage, the stress exponents are given at the top of the plot and the stresses at the bottom.

3. Results

3.1. Creep experiments

Fig. 1a and b shows the results of two creep tests corresponding, respectively, to one of each of the two sets of experiments. In Fig. 1a, one observes that stages 3 and 7 (deformed at 1300 °C) have a common extrapolation, as do 4, 6, and 8 (deformed at 1250 °C), indicating that the microstructure remains constant during creep, i.e. no dynamic grain growth

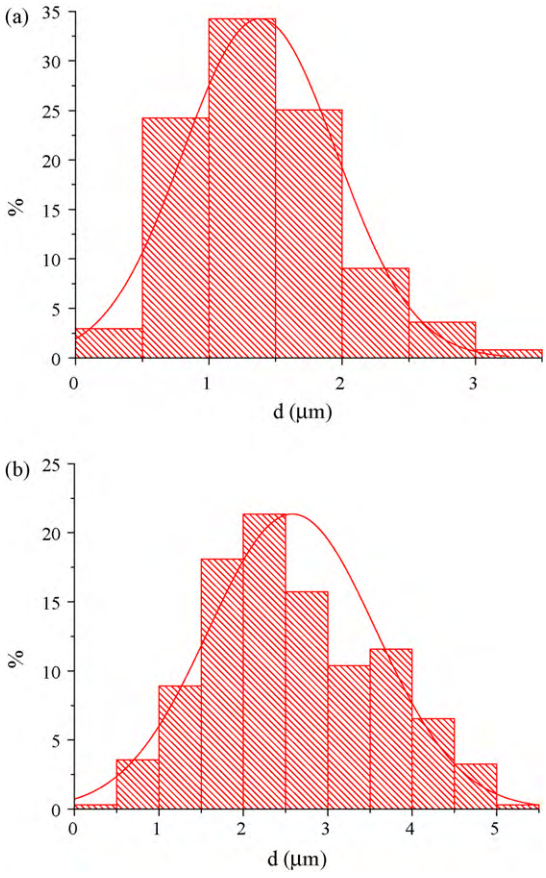

Fig. 2. Grain size histograms prior to (a) and after (b) deformation.

occurs. However, stages 1 and 5, and stages 2 and 4, 6, and 8 do not extrapolate, indicating that during the first two stages of creep the microstructure is evolving towards the final grain size (2.60 μm) as reflected by the changed microstructure observed after deformation. One can conclude therefore that the creep experiment is performed at constant microstructure from stage 3 onwards.

The values of the activation energies and stress exponents are, within the experimental error, $Q = 550 \pm 50$ kJ/mol and $n = 1.0 \pm 0.2$. The final elongation of all specimens was around 70%, and all of them deformed homogeneously.

3.2. Microstructural characterization of the post-mortem specimens

Equiaxially shaped grains were found to be a common feature in all samples. While grain size growth was observed after deformation, there were no changes in the grain aspect ratio. The grain size of the initial powder was 20 nm, and that of the ceramic material after the high-temperature treatment showed a major increase up to 1.4 μm as observed under SEM. After the creep tests, there was further significant grain growth, the new value being 2.60 μm (Fig. 2a and b).

A key feature of the grain size distribution was that the form factor did not change during creep. Table 1 illustrates this for as-received and post-mortem specimens.

Table 1
Form factor, average grain size, and their respective standard deviations, of ceria–zirconia ceramics before and after the creep test. A: before creep test, B: after creep test.

Sample	Shape factor	Standard deviation	Average grain size	Standard deviation
A	0.72	0.07	1.38	0.58
B	0.67	0.09	2.32	0.90
C	0.67	0.09	2.58	0.99

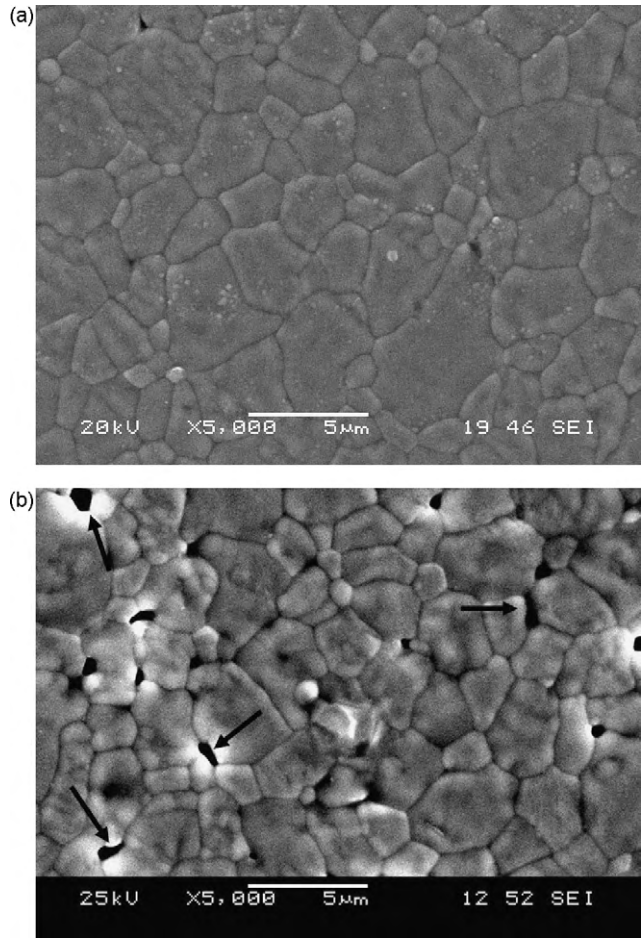

Fig. 3. SEM micrographs of as-received (a) and deformed (b) ceria–zirconia samples. Arrows point to the presence of cavities.

Fig. 3a and b is the SEM micrographs of the samples prior to and after deformation. The marked grain growth taking place during creep is evident. Moreover, grain accommodation during deformation is accompanied by the opening of cavities (arrows), an aspect required for grain boundary sliding, as will be discussed below.

4. Discussion

On the one hand, the experimental macroscopic values for both n and Q may in principle appear fully consistent with purely diffusional creep – Newtonian flow stress accommodated by bulk cation diffusion. Indeed, the values of the activation energy are in agreement with those found in superplastically

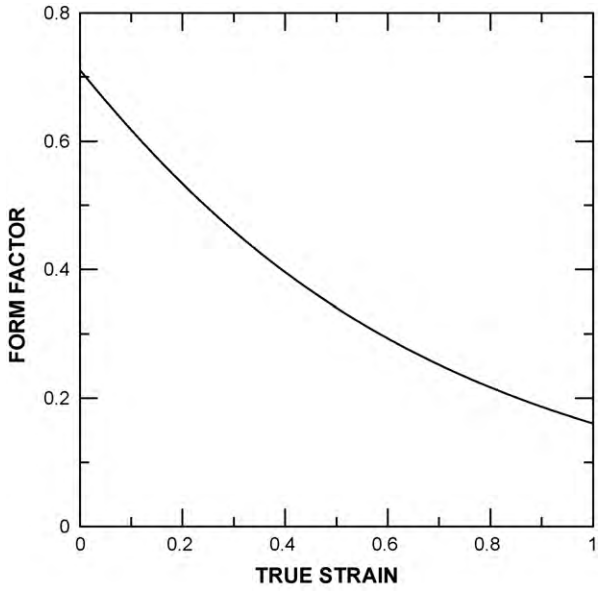

Fig. 4. Theoretical dependence of the form factor on the strain if deformation proceeds by diffusional creep only.

deformed YTZP in which cation defect diffusion controls the accommodation process.[2,7–9] A value similar to that reported here ($Q = 550 \pm 50$ kJ/mol) was found by Sakka et al.[10] in their determination of the activation energy for hafnium diffusion in ceria–zirconia ceramics. Their activation energies were 623 kJ/mol or 506 kJ/mol for lattice or grain boundary diffusion, respectively.

On the other hand however, the evolution of the microstructure shows that this picture must be discarded – diffusional creep demands a marked change in the form factors, since the driving force for deformation is pure mass transport from grain regions in compression to those in tension. Such a mechanism implies an anisotropic mass distribution. Since grains should evolve from equiaxial to ellipsoidal shapes, a simple theoretical analysis shows that the form factors should change from 0.72 in the initial stage to 0.25 when the final strain is 0.7. Fig. 4 is a plot of the form factor's dependence on strain if the deformation is entirely due to diffusional creep. Experimentally, however, the form factor changes only from 0.72 to 0.67, a variation that can account for at most 10% of the strain (see Fig. 4). The relative motion of two adjoining grains has components parallel and perpendicular to their common grain boundary. Grain boundary sliding (GBS) is the component parallel to the grain boundary and is responsible for 70–80% of the deformation, while the perpendicular motion is responsible for the accommodation processes needed during GBS. This has been reported to occur in superplastic fine-grained ceramics as evidenced by grain aspect ratio measurements at different strain stages and by atomic force microscopy.[11–13]

With diffusional creep thus delimited, the only mechanism left to appeal is that of Ashby–Verrall[14] with grain switching. This mechanism is consistent with the values of both the stress exponents and the activation energies, and can reasonably be assigned to the present case. Nonetheless, some aspects not considered in the original Ashby–Verrall model must be taken into account. First, the original model did not consider the possible role played by the curvature of the grain boundaries. One would expect this to be particularly relevant in fine-grained ceramics in which most grain boundaries adopt a rounded shape. Second, most studies of other zirconia ceramics, particularly those of yttria–zirconia ceramics, have reported that their high-temperature deformation mechanism fits the Ashby–Verrall picture with a stress exponent equal to 2 rather than the expected theoretical value $n = 1$. This inconsistency has quite recently been resolved with an improved modified version of the Ashby–Verrall model proposed by Gómez-García et al.[3] This new model predicts values of 2 or 1 depending on the grain size, stress, testing condition temperature, and the value of the test material's grain boundary energy. In particular, the stress exponent depends on the testing conditions according to the equation

$$n = \frac{2}{1+\beta} \tag{2}$$

where β is a dimensionless function of stress, the diffusion coefficients, and the grain boundary energy. In the framework of this model, the coefficient β can be estimated according to the expression

$$\beta = \frac{\pi}{8\alpha}\left(1 + \frac{\alpha^2}{4}\right)\frac{\sigma\delta}{\gamma}\frac{D_{\text{eff}}}{D_{\text{gb}}} \tag{3}$$

where α is a numerical constant close to 0.5 for almost equiaxially shaped grains, σ the applied stress, δ the thickness of the grain boundary diffusion layer, and γ the grain boundary energy. D_{eff} and D_{gb} are the effective diffusion and the grain boundary coefficients, respectively. The reasonable assumption has been made that the fastest diffusion path is the grain boundary path. Since $\sigma \approx 100$ MPa, $\delta \approx 5$ Å, and $\gamma \approx 0.1$ J m^{-2} in zirconia ceramics, this yields $\beta \approx 0.5$, and the corresponding value of the stress exponent is $n \approx 1.3$, which is very close to the experimental value. Unfortunately, this is not a complete validation of the applicability of the model. To the best of our knowledge, no data for the grain boundary energy are available and the value adopted in this estimate is for the current measurements in yttria–zirconia ceramics. It was also assumed that lattice diffusion proceeds quite rapidly in ceria–zirconia ceramics, much faster than in yttria–zirconia ceramics. These assumptions are reasonable but must be taken with caution while waiting for future experimental determinations against which to contrast the correctness of the application of the model[3] to ceria–zirconia ceramics. While such limitations need to be borne in mind, the model is useful to account for the main features of the high-temperature plasticity of ceria–zirconia ceramics. Grain boundary sliding is the leading mechanism controlling plasticity. Furthermore, the nonexistence of aliovalent cation segregation to the boundaries is consistent with an enhanced tendency for grain growth, a tendency which is in turn consistent with a stress exponent close to 1 according to the aforementioned model. This model predicts the appearance of cavities which close rapidly upon deformation. Under optimal superplastic conditions, there are only a few cavities. However, as deformation proceeds, this number no longer

remains constant, and cavitation increases progressively. This microstructural feature has been observed under SEM by Bravo-Leon et al.[15] in superplastically deformed yttria-stabilized zirconia, and under transmission electron microscopy (TEM) by Kim et al. in superplastic zirconia-dispersed alumina[16] and by Yasuda and Hiraga[17] in SiO_2-doped zirconia. Harjo et al.[18] and Ryukhtin et al.[19] have also observed the evolution of cavities during deformation under small-angle neutron scattering in YTZP. Their observations are coherent with the cavity opening observed in the SEM micrographs of our specimens (Fig. 3a and b).

5. Conclusions

We have described the compression creep test of a ceria–zirconia ceramic at high temperatures. The strain rates, stresses, and temperatures fitted the empirical creep equation with a Newtonian flow stress dependence and a purely Arrhenius temperature dependence. Both the microstructural features and the macroscopic parameters were explained in the framework of a modified version of the classical Ashby–Verrall model. This new version of the model had been shown to account for the existence of zirconia systems in which the stress exponent is 2 (such as yttria–zirconia systems) and also systems in which the linear dependence is maintained. The observed cavity formation during deformation is consistent with the main grain switching hypotheses proposed in that model.

Acknowledgements

Financial support granted by Spain's "Ministerio de Ciencia e Innovación" through projects MAT2009-14351-C02-01 and MAT2009-11078 is gratefully acknowledged.

Appendix A. Evolution of form factor with deformation during diffusional creep

The form factor is commonly defined as the ratio $F = 4\pi S/l^2$, where S is the section of the grain as observed under transmission electron microscopy (TEM), and l is the perimeter. As deformation proceeds, the rounded shape of the grains becomes elliptical. Let a and b denote the major and minor axes of the ellipse, with initial values (prior to deformation) a_0 and b_0. The minor axis is oriented along the direction of compression, and the major axis is usually normal to that direction.

Since the grain is becoming an ellipsoid and its volume does not evolve with time, the deformation dependence of a and b can be written as $a \propto \exp(\varepsilon/2)$ and $b \propto \exp(-\varepsilon)$, where ε is the true deformation. It is assumed that the macroscopic deformation is accounted for by the change of length of the compression axes in all the grains. This is fully consistent with the central hypothesis of diffusional creep.

A simple calculation of the surface area and length of an ellipse yields the following expression for the form factor:

$$F = 4\pi^2 \frac{b_0}{a_0} \times \frac{\exp(-(3/2)\varepsilon)}{\left[\int_0^{2\pi} \sqrt{1 - [1 - (1 - (b_0^2/a_0^2)\exp(-3\varepsilon))]\sin^2\theta}\, \mathrm{d}\theta\right]^2} \quad \text{(A.1)}$$

The ratio b_0/a_0 is determined by the initial value of F. The above function was plotted numerically using the MATHEMATICA software package, and is shown in Fig. 4.

References

1. Wakai F, Sakaguchi S, Matsuno Y. Superplasticity of yttria-stabilized tetragonal zirconia polycrystals. *Adv Ceram Mater* 1986;**1**:259–63.
2. Jiménez-Melendo M, Domínguez-Rodríguez A, Bravo-Leon A. Superplastic flow of fine-grained yttria-stabilized zirconia polycrystals: constitutive equation and deformation mechanisms. *J Am Ceram Soc* 1998;**81**:2761–76.
3. Gómez-García D, Zapata-Solvas E, Domínguez-Rodríguez A, Kubin LP. Diffusion-driven superplasticity in ceramics: modeling and comparison with available data. *Phys Rev B* 2009;**80**:214107-1–1214107-8.
4. Gómez-García D, Lorenzo-Martín C, Muñoz-Bernabé A, Domínguez-Rodríguez A. Correlation between yttrium segregation at the grain boundaries and the threshold stress for plasticity in yttria-stabilized tetragonal zirconia polycrystals. *Philos Mag A* 2003;**83**:93–108.
5. Gómez-García D, Lorenzo-Martín C, Muñoz-Bernabé A, Domínguez-Rodríguez A. Model of high-temperature plastic deformation of nanocrystalline materials: application to yttria tetragonal zirconia. *Phys Rev B* 2003;**67**:144101–7.
6. Gervais H, Pellicier B, Castaing J. Machine de fluage pour essais en compresión à hautes températures de matériaux céramiques. *Rev Int Hautes Temp Refract* 1978;**15**:43–7.
7. Dominguez-Rodriguez A, Gutierrez-Mora F, Jimenez-Melendo M, Routbort JL, Chaim R. Current understanding of superplastic deformation of Y-TZP and its application to joining. *Mater Sci Eng* 2001;**A302**:154–61.
8. Gutiérrez-Mora F, Domínguez-Rodríguez A, Jiménez-Melendo M, Chaim R, Hefetz M. Creep of nanocrystalline Y-TZP ceramics. *Nanostruct Mater* 1999;**11**:531–7.
9. Winnubst AJA, Boutz MMR, He YJ, Burggraaf AJ, Verweij H. Plasticity of nanocrystalline zirconia ceramics and composites. *Ceram Int* 1997;**23**:215–21.
10. Sakka Y, Oishi Y, Ando K, Morita S. Cation interdiffusion and phase stability in polycrystalline tetragonal ceria–zirconia–hafnia solid solution. *J Am Ceram Soc* 1991;**74**:2610–4.
11. Ishihara S, Tanizawa T, Akashiro K, Furushiro N, Hori S. Stereographic analysis of grain boundary sliding in superplastic deformation of alumina–zirconia two phase ceramics. *Mater Trans JIM* 1999;**10**:1158–65.
12. Duclos R, Crampon J, Carry C. Grain boundary sliding and accommodation mechanism during creep of yttria-partially stabilized zirconia. *Philos Mag Lett* 2002;**82**:529–33.
13. Duclos R. Direct observation of grain rearrangement during superplastic creep of a fine-grained zirconia. *J Eur Ceram Soc* 2004;**24**:3103–10.
14. Ashby MF, Verrall RA. Diffusion-accommodated flow and superplasticity. *Acta Metall* 1973;**21**:149–63.
15. Bravo-Leon A, Jiménez-Melendo M, Domínguez-Rodríguez A. Mechanical and microstructural aspects of the high temperature plastic deformation of yttria-stabilized zirconia polycrystals. *Acta Metall Mater* 1992;**40**:2717–26.
16. Kim BN, Hiraga K, Sakka Y, Jang G. Effect of cavitation on superplastic flow of 10% zirconia-dispersed alumina. *Scripta Mater* 2001;**45**:61–7.

17. Yasuda HY, Hiraga K. Cavity damage accumulation and fracture in SiO_2-doped zirconia during superplastic deformation. *Mater Sci Eng* 1997;**A234–A236**:343–6.
18. Harjo S, Kojima N, Motohashi Y, Šaroun J, Ryukhtin V, Strunz P, et al. Characterization of cavities in superplastically deformed tetragonal zirconia polycrystals by means of small angle neutron scattering. *Mater Trans* 2002;**43**:2480–6.
19. Ryukhtin V, Šaroun J, Harjo S, Motohashi Y, Baron M, Loidl R. Comparative study of porosity in 3Y-TZP superplastic ceramics by USANS and SEM image analysis. *J Appl Cryst* 2003;**36**:478–83.